J Mater Sci (2010) 45:2099–2105
DOI 10.1007/s10853-009-3924-7

HTC2009

Non-reactive versus dissolutive wetting of Ag–Cu alloys on Cu substrates

O. Kozlova · R. Voytovych · P. Protsenko · N. Eustathopoulos

Received: 30 June 2009 / Accepted: 23 September 2009 / Published online: 27 October 2009

Abstract The fundamental issues of equilibrium and non-equilibrium (dissolutive) wetting and spreading in the liquid Ag/solid Cu system are studied by the dispensed drop technique. To this end, wetting experiments of Cu, both mono- and poly-crystalline, with two types of Ag–Cu alloys, one non-saturated and the other saturated in copper, are performed at 900 °C in high vacuum by the dispensed drop technique. The results are compared with those given in the literature for the same or similar systems as well as with model predictions.

Introduction

In any liquid metal A/solid metal B system there is a range of temperatures where the main reaction occurring at the solid/liquid interface is dissolution of the solid into the liquid. When the solubility in the liquid phase is high, dissolution of solid B into a droplet of metal A leads to a macroscopically non-planar interface. "Dissolutive wetting" is of great interest both for fundamental research and for several industrial processes, an important example being soldering in microelectronics fabrication [1]. Several studies performed with the molten Sn/solid Bi model system have shown that dissolution improves wetting, i.e. it increases the area of contact between the two phases [2–4]. The spreading time in dissolutive wetting (defined as the time needed for millimetre-sized droplets to attain a capillary equilibrium) in this and similar systems are from a few seconds to several hundred seconds [2–7]. This time is several orders of magnitude higher than the spreading time found in metal A/metal B systems with negligible miscibility, which is typically around 10 ms [8–11]. From modelling of dissolutive spreading, performed in [3], it was concluded that in the Sn/Bi system both the configuration at the solid/liquid/vapour triple line and the spreading rate were controlled by diffusion of dissolved species from the interface to the liquid bulk. However, this approach does not take into account the role in wetting of the change in surface energies of the solid/liquid/vapour system caused by dissolution. For instance, as the surface tension of liquid Bi is 35% lower than that of Sn [10], the dissolution of Bi is expected to modify the surface tension of the liquid thus also affecting the wetting process. A similar situation exists during Si dissolution in molten Cu [7].

In both Sn/Bi and Cu/Si systems mentioned above, the solubility of the liquid metal (Sn or Cu) in the solid (Bi and Si, respectively) is negligible. In a recent study performed by the "transferred drop technique" for the fully miscible couple Au/Ni (as well as for the Cu/Ni and Ge/Si couples) a very fast spreading regime was found [11]. The spreading time in the Au/Ni system was close to 15 ms, i.e. typical of immiscible metal/metal systems [11]. Surprisingly, no specific dissolutive wetting stage was found to occur at longer times. However, the authors of this study reported the presence of a continuous, submicronic thick film on the substrate surface, extending hundreds of microns ahead of the drop and this was interpreted as a Marangoni film.

The study reported in the present paper concerns the Ag/Cu system presenting a notable solubility of Ag in solid Cu (Fig. 1). Wetting experiments are performed at 900 °C on pure copper substrates with two liquid Ag–Cu alloys, one

O. Kozlova · R. Voytovych (✉) · N. Eustathopoulos
SIMaP/PHELMA, INPG, D.U., BP 75, 38402 St. Martin d'Hères, France
e-mail: rayisa.voytovych@simap.grenoble-inp.fr; rvoytovych@yahoo.de

P. Protsenko
Department of Colloid Chemistry, MSU, Moscow, Russia

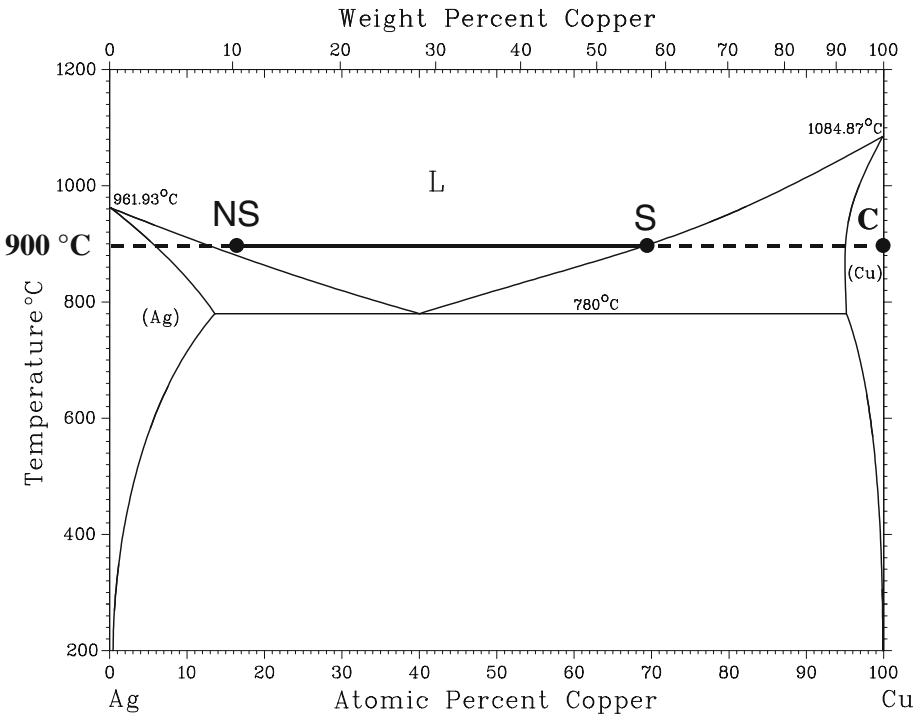

Fig. 1 Ag–Cu phase diagram [12]. The two alloy compositions used in the present study are noted NS (non-saturated alloy) and S (saturated alloy). In all experiments the solid substrate was pure Cu

non-saturated in Cu (hereafter referred to as NS), the other saturated in this metal (hereafter referred to as S). The liquid Ag/solid Cu system was investigated previously in two studies carried out in order to assess the fundamental characteristics of non-equilibrium (dissolutive) wetting and spreading. In the first of these studies, Sharp et al. [13] carried out sessile drop experiments for various equilibrium and non-equilibrium conditions of solid and liquid phases. However, in the sessile drop technique used in these experiments, the initial stages of spreading were obscured by metal melting. In the present study this difficulty is overcome by using the dispensed drop technique which enables the processes of melting and spreading to be separated [7]. More recently, Webb et al. [14] studied wetting of solid Cu by liquid Ag and Ag–Cu using molecular dynamics simulation applied to very small droplets, a few nanometres in size. They concluded that in dissolutive wetting the drop base diameter increases with time parabolically. These authors argued that the conclusions drawn from this type of calculation can be extrapolated to macroscopic droplets.

The liquid compositions used in the present study are given in Fig. 1. The mole fraction of Cu in the NS liquid is slightly higher than that of the Ag liquidus at 900 °C ($x_{Cu} = 0.125$). During a wetting experiment, Cu substrate dissolution leads to the liquid composition denoted as S in Fig. 1 ($x_{Cu} = 0.70$). Dissolution will create a crater of volume V_{cr} under the drop. For a volume V_0 of an NS droplet, V_{cr} can be easily calculated from the mole volumes of the saturated and non-saturated liquids and of solid Cu. The calculation yields $V_{cr} = 1.27V_0$. The change in alloy composition during dissolution results in a limited but significant increase in the surface tension, by about 6% [15]. For alloy S, saturated in Cu, only diffusion of Ag from the liquid droplet into solid Cu is expected to occur during a sessile drop experiment.

Experimental procedure

Wetting was studied by the dispensed drop method, in a metal furnace under a vacuum of 5×10^{-5} Pa. The experiment involves heating an Ag–Cu alloy (purity > 99.99%) in an alumina crucible placed above the Cu substrate. At the experimental temperature, 900 °C, the liquid was extruded from the crucible through a capillary and put in contact with a Cu substrate, either mono- or poly-crystalline, with an average surface roughness of 1–4 nm. The initial diameter of the droplets d_{dr} was between 1.0 and 1.3 mm.

The wetting was filmed by a high-speed camera (500 frames per second) allowing the process to be recorded over a 4-s period. Selected experiments were subsequently filmed with 25 frames per second in order to follow the spreading process for a longer time. The camera was connected to a computer for automatic image analysis. The characteristic dimensions of the drop (drop base diameter d and visible contact angle θ) were extracted with an accuracy of $\pm 2°$ for θ and $\pm 2\%$ for d. Note, however, that during the very first moments of spreading (at $t < 5$ ms),

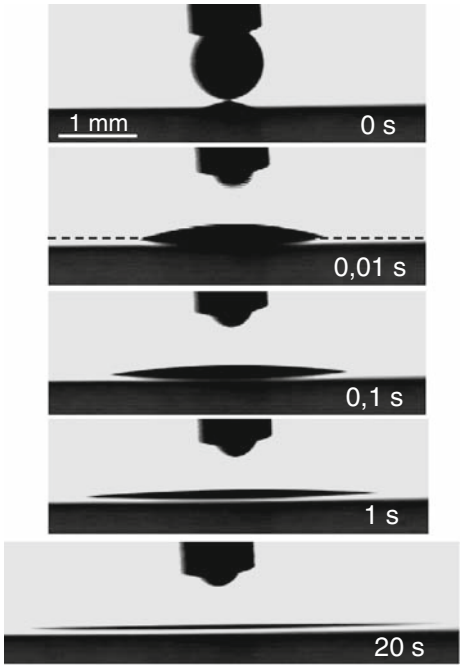

Fig. 2 Selected images of spreading of an S alloy on monocrystalline Cu. The *dashed line* shows the position of the interface

when the triple line velocity is very high (close to 0.5 m/s), the error on θ was estimated to be $\pm$ 5°. At $t > 0.5$ s the contact angle θ becomes lower than 5° (Fig. 2). For such small contact angles an accurate measurement of θ on a drop profile is difficult. At $t > 20$ s even the determination of the position of the triple line becomes difficult and may introduce a high degree of error on the drop base diameter value. In order to evaluate this error, the final diameter was measured both by image analysis and directly on the solidified droplet. The difference between these two values was found to be less than 5%.

After cooling, selected specimens were cut perpendicular to the interface for SEM observation and EDXS analysis.

Results

Spreading kinetics

Figure 3 presents the drop base diameter d and contact angle θ as a function of time plotted on a logarithmic scale for two S and two NS drops spreading on the surface of monocrystalline Cu substrates at 900 °C. Diameter d was normalised by $d_{dr} = (6\ V/\pi)^{1/3}$ where V is the initial drop volume. As seen in Fig. 3a, the spreading curves are nearly superimposed up to about 20–30 ms implying that, during this initial period of time, spreading is not linked to substrate dissolution and may be attributed to non-reactive wetting. After 30 ms, the spreading of the non-saturated drops becomes faster than for the saturated drops leading to higher drop base diameters for the NS drops.

Similar results were obtained with polycrystalline Cu substrates confirming the main finding, namely, that the spreading rate is higher for the NS liquid than for the S liquid. As a result, the drop base radius of NS alloys after 1 s of spreading is 20–40% higher than for S alloys, depending on the experiment.

It should be noted that the spreading curves presented in Fig. 3 did not attain a stationary state. Indeed, the drop base diameter continues to grow as shown in Fig. 4 for two drops (one S and one NS) filmed until they reached a steady drop base diameter. In both cases the spreading time slightly exceeded 100 s. The final contact angles θ_F are very close to zero ($0 < \theta_F < 2°$). The comparison of Figs. 3 and 4 shows that the difference in drop diameter between NS and S droplets becomes constant as spreading proceeds.

Based on these observations, the faster spreading of the NS liquid in the time interval between 0.03 and $\sim$1 s is attributed to dissolution of Cu into the molten Ag–Cu alloy. Further evidence of this statement will be given below.

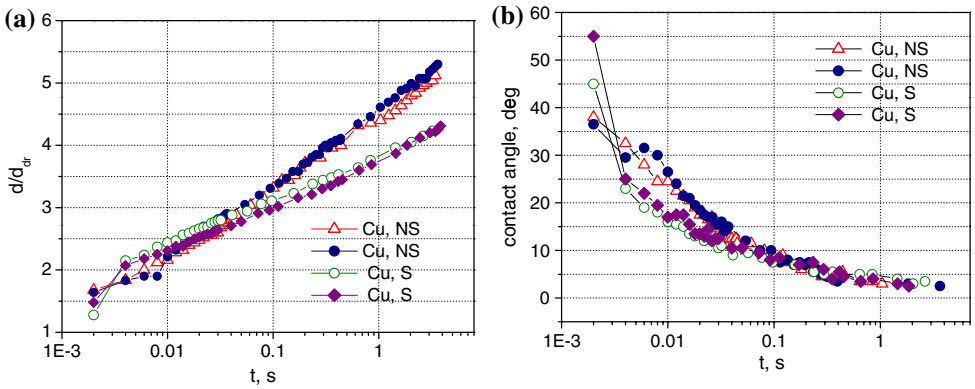

Fig. 3 Normalised drop base diameter (**a**) and contact angle (**b**) as a function of logarithm of time for two S and two NS Ag–Cu drops spreading on monocrystalline Cu at $t < 4$ s

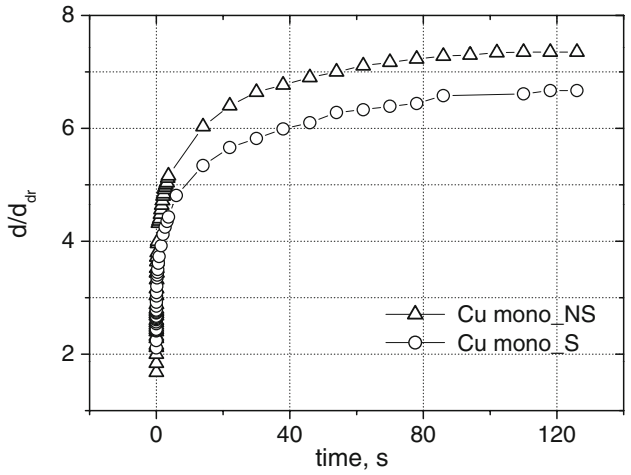

Fig. 4 Normalised drop base diameter as a function of time for saturated S and non-saturated NS alloys on monocrystalline Cu (experiments followed until capillary equilibrium)

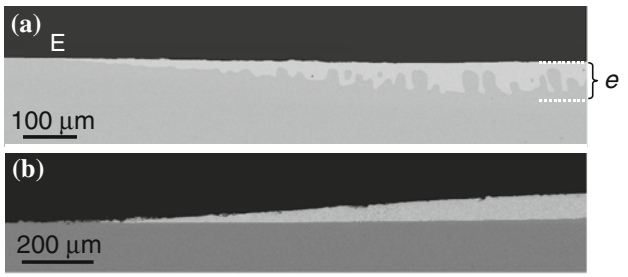

Fig. 5 Cross-section of NS (**a**) and S (**b**) drops on monocrystalline Cu. The holding times at 900 °C are 690 and 60 s, respectively. *E* indicates the edge of the crater formed by NS drop

Characterisation of solidified droplets

SEM observations of cross-sections of a sample obtained for a NS alloy show the formation of a crater in the Cu substrate (Fig. 5a). The crater diameter is considerably smaller than that of the final drop and corresponds approximately to the drop base diameter after 0.7–1 s of spreading, depending on the experiment. In the middle of the crater, the thickness *e* of the liquid is close to 100 µm and it decreases progressively to a few tens of microns at its edge (point E in Fig. 5a).

Outside the crater, the drop extends over a distance of 2–3 mm, forming a liquid film the thickness of which gradually decreases from a few tens of microns at the crater edge towards zero at the triple line. Figure 6 shows overhead views of this layer in the vicinity of the crater (a) and some 1600 µm away from it (b) for a Ag–Cu drop held for 690 s at 900 °C. To understand the observed patterns, the diffusion of Ag from the liquid film into solid Cu must be taken into account. This diffusion results in the formation of primary Cu at the experimental temperature (isothermal

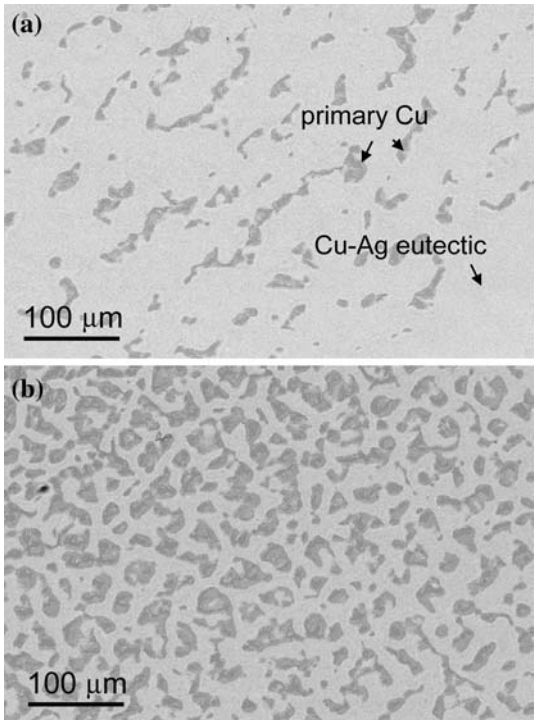

Fig. 6 Overhead views of a solidified droplet formed by an NS alloy on a Cu substrate: in the vicinity of the crater (**a**) and about 1600 µm away from it (**b**). The holding time at 900 °C is 690 s

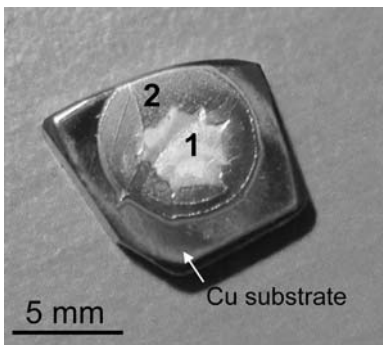

Fig. 7 Overhead view of an NS solidified droplet on a Cu single crystal. 1 and 2 are parts of the solidified droplet: 1 shows the zone above the dissolution crater and 2 the zone of liquid film (see also Fig. 8). The holding time at 900 °C is 690 s

solidification). Moving further out from the crater edge, the liquid thickness decreases and the fraction of primary Cu on the surface increases.

Figure 7 presents an overhead view of an NS droplet maintained at 900 °C for 690 s. A central, rich in Ag, drop area corresponding to the crater formed during the dissolutive stage, and a peripheral region, corresponding to the liquid film where the formation of Cu dendrites led to a change in the drop colour is clearly visible.

Figure 5b shows the SEM micrographs of an S alloy/Cu solid cross-section. As expected for a Ag–Cu liquid alloy

saturated in copper, the solid Cu/liquid interface remains flat. As for the solidified alloy, it consists of Cu–Ag eutectic and Cu rich dendrites.

Discussion

Figure 8a presents schematically the three spreading sequences evidenced for NS liquid on Cu monocrystals. The second, dissolutive stage results in the formation of a crater under the drop and in saturation of the liquid with Cu. In the third stage, spreading outside the crater proceeds without dissolution, only diffusion of Ag into solid Cu occurs.

The results for the Ag/Cu system are compared in Table 1 with those for the Cu/Si system obtained previously by the dispensed drop technique at 1100 °C using (111) Si single crystals [7]. For the saturated alloys, the spreading time t_{spr} for the Ag/Cu couple (noted S-Ag/Cu) is four orders of magnitude higher than for the S-Cu/Si system. This considerable difference is not due to the different experimental temperatures (900 °C against 1100 °C) or to differences in the dynamic properties of the two saturated liquid alloys. Indeed, as shown by Fig. 3a contact angle of 22° is attained for the S-Ag/Cu couple in a few ms, just like the S-Cu/Si couple. The difference in t_{spr} is certainly due to the very different equilibrium contact angles θ_F of these systems: 22° against only (about) 1°. As indicated by the shape of θ (log t) and $d(t)$ curves (Figs. 3b and 4), the spreading rate decreases dramatically when θ tends towards very small values. The behaviour found in the present study for the S-Ag/Cu system, i.e. long time spreading without the occurrence of a significant reaction between the solid and liquid phases, could also be observed for any liquid metal forming very low equilibrium contact angles. As discussed in [10], such systems may be metal/metal couples with a small difference in composition between the solid and liquid phases implying a low solid–liquid interfacial energy. An example is Ni-11 wt% P droplets spreading at 1020 °C over pure Ni for several hundred of seconds [6].

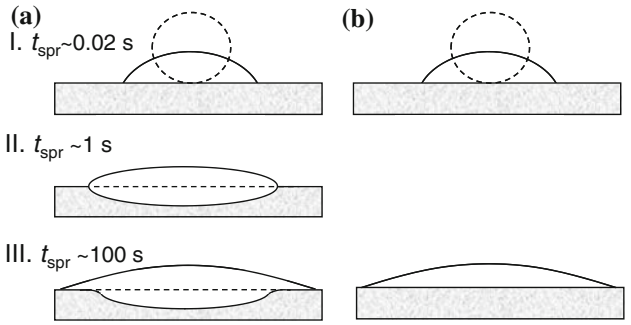

Fig. 8 Schematic presentation of the spreading stages for NS (**a**) and S (**b**) Ag–Cu alloys on solid Cu. Stages I and III correspond to non-reactive spreading while stage II is the dissolutive stage

Table 1 Spreading regimes in NS (Ag-rich alloy)/solid Cu system

Time interval (s)	Drop base diameter (d/d_{dr}) evolution	Spreading regime	Average spreading rate (m/s)
0–0.03	0–2.6	Non-reactive	10^{-1}
0.03–1	2.6–4.6	Dissolutive	10^{-3}
1–100	4.6–7.3	Diffusion into the solid	10^{-5}

$T = 900$ °C

The differences in the θ_F of S alloys can also explain the different final configurations observed for NS alloys in the two systems, with and without a liquid film outside the dissolution crater (Table 1). For the NS -Ag/Cu couple, at the end of the dissolutive stage, occurring at $t \approx 1$ s, the contact angle is close to 4°, which is still higher than the equilibrium contact angle ($\approx 1°$). As a consequence, spreading can continue outside the crater forming the observed liquid film. In contrast, for the NS-Cu/Si couple, the contact angle at the end of the dissolutive stage is 6°, lower than the equilibrium contact angle of 22°. As a result, no further spreading of the liquid on the flat solid substrate outside the crater can occur in this case. From the above analysis, it can be seen that while in the Cu/Si system non-reactive spreading and dissolutive spreading are two successive stages with different time scales, in the Ag/Cu system non-reactive spreading occurs not only before ($t < 0.02$ s) but also after ($t > 1$ s) the dissolutive stage. Note that the configuration III in Fig. 8a was observed previously in the Sn/Au system at 430 °C and was explained by the nearly perfect wetting of Sn on Au induced by the formation at the interface of an Au rich Au–Sn intermetallic compound [5].

The results described in the diagram of Fig. 8 do not match those given in [11] for the Au/Ni system (a fully miscible system for which a very small equilibrium contact angle is expected to form as indicated above). Indeed, even if the liquid films observed in our study can be compared with those reported for the Au/Ni system, the explanation given for their origin is very different: Marangoni films extending ahead of the drop (in [11]) and primary wetting films (present study). Moreover, while the total spreading time in our study was found to be as long as 100 s, in [11] it was only 15–20 ms, i.e. typical of the spreading time in immiscible systems. Note that in the transferred drop technique used in [11], the excess energy liberated during drop detachment from the auxiliary substrate and its transfer to the substrate under study, can disturb the spreading process and affect the results (see for instance the results of [8] reported also in [10]).

Figure 9 shows the variation in drop base radius R with time, in a log–log presentation, for the two Ag–Cu alloys, one NS, the other S, both on monocrystalline Cu. For the S alloy, all the results obtained for the time interval between 10^{-2} and 10^{2} s can be described by a single straight line LL′ corresponding to $R^n \sim At$ with $n = 9.78$. A second experiment with an S alloy led to $n = 9.26$. Both n values are close to the theoretical value $n = 10$ predicted by the hydrodynamic model of spreading assuming that spreading is limited by the viscous dissipation in the drop bulk [16, 17]. As for the constant A, its value, calculated from the slope of the straight line, is 4×10^{-28} against a theoretical value of 8×10^{-27}. The latter value was calculated using the expression $A = \frac{3V^3\sigma}{\eta K}$ taking for drop volume $V = 5 \times 10^{-10}$ m, the viscosity $\eta = 4.3 \times 10^{-3}$ Pa s [18] (Table 2), surface tension $\sigma = 0.95$ N/m [14] and for the parameter K (an empirical model constant) $K = 10$ [16]. Even taking $K = 16$, which is the maximum value of this parameter with a physical meaning, the theoretical value A remains one order of magnitude higher than the experimental value. The overestimation of the spreading rate of low viscosity liquids by the hydrodynamic model has been

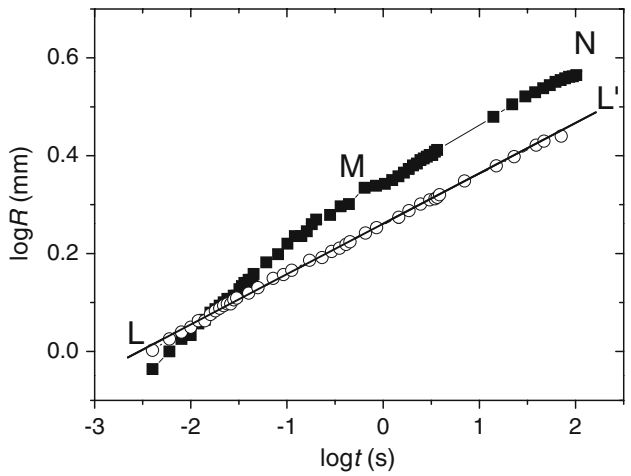

Fig. 9 Drop base radius R as a function of time in log–log presentation for S (*open circles*) and NS (*filled squares*) alloys spreading over monocrystalline Cu

Table 2 Data on the physico-chemical properties in liquid Ag–Cu/solid Cu system

Drop base radius after non-reactive wetting, r_0	1.3E−03	m
$\Delta\sigma$	0.05	N/m
Cu–Ag alloy density[a], ρ_{Ag-Cu}	9.80E+03	kg/m^3
Equilibrium contact angle, θ_Y	13	deg
Cu–Ag alloy viscosity[b], η	4.3E−03	N s/m^2

$T = 900$ °C

[a] Average values for Ag-12.5 at.%Cu and Ag-58 at.%Cu

[b] Viscosity value for eutectic alloy

recognised both for room temperature liquids [19, 20] and for molten metals [11]. In [11, 19] it was argued that this overestimation is due to the fact that, for this type of liquid, the dissipative process in the vicinity of the triple line described in Blake's model [21] is also significant if not predominant. However, when the process at the triple line is predominant, the exponent n is no longer equal to 10 but its value is close to 7 [19].

For the non-saturated alloy, dissolution enhances the spreading rate. Indeed, the average spreading rate $\overline{U}_{spr}$ for the NS alloy in the time interval between 0.03 and 1 s is 0.9 mm/s, ~70% higher than $\overline{U}_{spr}$ for the S alloy during the same period. This cannot be explained by the change in the σ/η ratio affecting the rate of viscous spreading. Indeed, using experimental data for σ [15] and η [18] of Cu–Ag alloys, it can be seen that this ratio for the NS alloy is lower than for S alloy. The increase in $\overline{U}_{spr}$ due to dissolution may be caused by the solutocapillary (Marangoni) convection generated by the variation in surface tension $\Delta\sigma$ between the top of the drop, where the liquid is rich in Ag and its surface tension comparatively low, and the triple line where the liquid is rich in copper and its surface tension comparatively high (Fig. 10). An order of magnitude of the initial convective velocity U_{conv} of the liquid induced by the σ gradient at the beginning of the dissolutive process can be calculated from a balance between surface tension and viscous forces as $U_{conv} \approx \frac{\Delta\sigma \cdot \sin\theta}{\eta}$ [22]. With $\Delta\sigma = 0.05$ N/m and $\theta = 13°$ (Table 2) a value of $U_{conv} \approx 2$ m/s is obtained. Such a value is certainly an overestimation, since with such a high velocity; inertia should be taken into account in the force balance. Nevertheless, it can be safety stated that the fluid flow is quite intense within the drop. It is worth noting that, by both model calculations and experimentally with organic liquids [23], it was found that thermocapillary convection can affect spreading limited by viscous friction. There is no reason why solutocapillary convection should not have a similar effect.

A final remark concerns the comparison between our results and those of Webb et al. [14], obtained by simulation for Ag nanodroplets on Cu. For the dissolutive stage (straight line LM of the curve in Fig. 9), n lies between 0.14 and 0.17 depending on the experiment. This is much

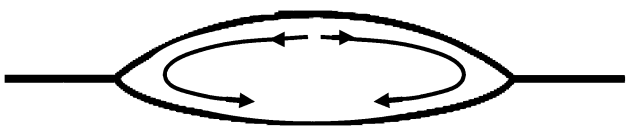

Fig. 10 Solutocapillary convection pattern in an Ag-rich droplet on a Cu substrate. Convection is driven by the difference in surface tension σ between the top of the drop (low σ) and the triple line region (high σ)

lower than the value 0.5 found by Webb et al. Note that the spreading rates computed by Webb were several m/s, i.e. three orders of magnitude higher than the spreading rates measured in the present study for the dissolutive stage. This indicates that either the results given in [14] concern the initial, non-reactive stage of spreading rather than the dissolutive stage or that the drop size has a very strong effect on spreading kinetics.

Conclusions

In the present work, the equilibrium and non-equilibrium spreading of Ag–Cu alloys over solid Cu at 900 °C were studied. The key factor for the spreading kinetics in this system is the nearly zero equilibrium contact angle. This leads to a spreading time t_{spr} for the Cu-saturated liquid several orders of magnitude higher than t_{spr} measured previously in metal/metal systems with contact angles lying in the range 20–50°. The drop base radius R decreases with time according to a power law $R^n \sim At$ with n lower than but close to 10 which strongly suggests that spreading is limited by viscous dissipation. However, it is not clear if the dissipative process occurs only in the drop bulk or also at the triple line. Furthermore, the very small contact angle and the slow spreading kinetics are responsible for the configuration observed during non-equilibrium (dissolutive) spreading consisting in a central crater and a liquid film spreading on the flat substrate surface outside the crater. Dissolution of copper in the drop increases the spreading rate significantly (factor 1.7). This effect is attributed to the solutocapillary (Marangoni) convection induced by differences in surface tension between the top of the drop (low σ) and the triple line region (high σ). It is expected that the conclusions drawn in the present study will also be valid for a metal/solid metal system with total miscibility in the liquid and a significant solubility of the solid.

Acknowledgements The authors would like to thank Dr. J.-P. Garandet for interesting discussions on this topic.

References

1. Boettinger WJ, Handwerker CA, Kattner UR (1993) In: Yost FG, Hosking FM, Frear DR (eds) The mechanics of solder alloy wetting and spreading. Kluwer Academic Publishers, Boston
2. Yost FG, O'Toole EJ (1998) Acta Mater 46:5143
3. Warren JA, Boettinger WJ, Roosen AR (1998) Acta Mater 46:3247
4. Yin L, Murray BT, Singler TJ (2006) Acta Mater 54:3561
5. Yin L, Meschter SJ, Singler TJ (2004) Acta Mater 52:2873
6. Ambrose JC, Nicholas MG, Stoneham AM (1993) Acta Metall Mater 8:2482
7. Protsenko P, Kozlova O, Voytovych R, Eustathopoulos N (2008) J Mater Sci 43:5669. doi:10.1007/s10853-008-2814-8
8. Naidich YuV, Zabuga VV, Perevertailo VM (1992) Adgeziya rasplavov i paika materialov 27:23 (in Russian)
9. Ebrill N, Durandet Y, Strezov L (2001) Trans JWRI 30:351
10. Eustathopoulos N, Nicholas M, Drevet B (1999) Wettability at high temperature, Pergamon materials series, vol 3. Pergamon, Oxford
11. Saiz E, Tomsia AP (2004) Nat Mater 3:90
12. Massalski TB (ed) (1990) Binary alloy phase diagrams, 2nd edn. ASM International, Metals Park, Ohio
13. Sharps PR, Tomsia AP, Pask JA (1981) Acta Metall 9:855
14. Webb EB III, Grest GS, Heine DR, Hoyt JJ (2005) Acta Mater 53:3163
15. Bricard A, Eustathopoulos N, Joud JC, Desré P (1973) CR Acad Sci Paris 276:1613
16. de Gennes PG (1985) Rev Mod Phys 57:827
17. Cox RG (1986) J Fluid Mech 11:714
18. Battezzati L, Greer AL (1989) Acta Metall 37:1791
19. De Coninck J, de Ruijter M, Voué M (2001) Curr Opin Colloid Interface Sci 6:49
20. Cazabat AM, Gerdes S, Valignat MP, Villette S (1997) J Colloid Interface Sci 5:129
21. Blake TD (1993) Dynamic contact angles and wetting kinetics. Marcel Dekker, New York
22. Camel D, Tison P, Garandet JP (2002) Eur Phys J 18:201
23. Ehrhard P (1993) J Fluid Mech 257:463